CHEMICAL ENGINEERING TRANSACTIONS
VOL. 50, 2016
A publication of AIDIC
The Italian Association of Chemical Engineering
Online at www.aidic.it/cet
Guest Editors: Katharina Kohse-Höinghaus, Eliseo Ranzi

ISBN 978-88-95608-41-9; **ISSN** 2283-9216
DOI: 10.3303/CET1650009

A CFD Model for Biomass Flame-Combustion Analysis

Giancarlo Gentile*, Paulo E.A. Debiagi, Alberto Cuoci, Alessio Frassoldati, Tiziano Faravelli, Eliseo Ranzi

Politecnico di Milano; Dipartimento di Chimica, Materiali e Ingegneria Chimica "Giulio Natta", Piazza Leonardo Da Vinci, 32; 20133 Milano; Italia
giancarlo.gentile@polimi.it

The present work addresses the study of the combustion of individual biomass particle surrounded by a gas stream of N_2/O_2 under the operating conditions encountered in a drop tube reactor. The aim of this analysis is to give a better insight into the chemical and physical processes that occur both at particle and reactor scale where the volatiles, generated by the biomass pyrolysis, burn in a fuel particle enveloped flame.
A comprehensive CFD model was developed within the open-source OpenFOAM® framework in order to properly handle the computational mesh and the discretization of the characteristic governing equations. At the reactor scale, the reactive flow was described by the equations for continuous, multicomponent, compressible and thermally-perfect mixtures of gases. At the particle scale, instead, the solid particle was considered as a porous media with isotropic and uniform morphological properties.

1. Introduction

Since the beginning of the age of industrialization, the social and economic development has resulted in an accelerating demand in energy and resources. Up to now, fossil fuels have made a large contribution to the energy systems exploitation. Currently, more than 80% of the world energy supply is still based on fossil fuels, but such a condition cannot be accepted in a long-term scenario. In this context, a growing interest in biomass fuels spread around the scientific community. Biomass, such as woods and agricultural residues, is an attractive fuel for power generation because is widely available, easily accessible at relatively low costs and characterized by a reasonable energy density. There are three principal ways to release heat and energy from biomass: direct combustion, gasification and pyrolysis. Pyrolysis results hierarchically the most important, because it is the first step also during both gasification and combustion.
Several researchers have developed models for biomass pyrolysis at particle scale (Corbetta et al., 2014, Bates and Ghoniem, 2014). These models couple the kinetics of primary and secondary pyrolysis with the concomitant description of the heat and mass transport phenomena. Most of these models are one-dimensional in space and assume local thermal equilibrium between the solid and gas species.
In a previous work, we have successfully proposed a new numerical framework, named bioSMOKE (Gentile et al., 2015), based on the OpenFOAM® (OpenFOAM) framework able to efficiently perform Computational Fluid Dynamics (CFD) simulations of pyrolysis of biomass at the particle scale.
In a typical pyrolysis device, biomass devolatilization is strongly influenced by the fluid dynamic of the surrounding gas that specifically affects the process of thermal degradation. Therefore, in order to achieve an accurate description of the reacting system behavior, the dynamic of biomass particle decomposition must be coupled with the modeling of the surrounding fluid phase.
For these reasons, here we extend the previously developed numerical tool to account the fluid phase reacting system. In particular, in order to couple the solution of the transport equations in the fluid phase with the transport phenomena in the solid one, a multiregion model has been considered. The whole computational domain is split in different regions, which are characterized by different phenomena and governing equations. A similar approach has been adopted elsewhere (Maffei et al., 2016).
The paper is structured as follows. In Section 2, we provide a detailed description of the governing equations both at the particle and the reactor scale with a comprehensive detail of the numerical method and its applications with OpenFOAM®. In the Section 3, we present a showcase of pyrolysis of a particle of

Please cite this article as: Gentile G., Debiagi P.E.A., Cuoci A., Frassoldati A., Faravelli T., Ranzi E., 2016, A cfd model for biomass flame-combustion analysis, Chemical Engineering Transactions, 50, 49-54 DOI: 10.3303/CET1650009

sugarcane-bagasse in order to validate the method and to test reliability, efficiency and limitations of the new solver.

2. Mathematical formulations

The mathematical model for the biomass pyrolysis is based on the fundamental governing equations of conservations of total mass, momentum and energy for both fluid and solid phases.

2.1 Governing equations of solid phase

The solid phase is considered as a porous medium including both the solid volume and the fluid contained inside its pores. In this the particle shrinking has been neglected. The conservation equations are written as shown in the following.

$$\frac{\partial}{\partial t}\left(\rho^G \varepsilon\right)+\nabla\left(\rho^G \mathbf{u}\right)=\dot{\Omega} \tag{1}$$

$$\frac{\partial}{\partial t}\left(\rho^G \varepsilon \mathbf{u}\right)+\nabla\left(\rho^G \mathbf{u}\mathbf{u}\right)=-\nabla p+\nabla\cdot\left[\mu\left(\nabla\mathbf{u}+\nabla\mathbf{u}^T\right)-\frac{2}{3}\mu\left(\nabla\mathbf{u}\right)\mathbf{I}\right]+\rho^G\mathbf{g}+\mathbf{S} \tag{2}$$

$$\frac{\partial}{\partial t}\left(\rho^G \varepsilon \omega_k\right)+\nabla\left(\rho^G \omega_k \mathbf{u}\right)=-\nabla j_k+\dot{\Omega}_k \qquad k=1,\ldots,NC_{gas} \tag{3}$$

$$\frac{\partial}{\partial t}\left(\rho^S\left(1-\varepsilon\right)\omega_j\right)=\dot{\Omega}_j \qquad j=1,\ldots,NC_{solid} \tag{4}$$

$$\hat{C}_p^{gas}\frac{\partial\left(\rho^G\varepsilon T\right)}{\partial t}+\hat{C}^{solid}\frac{\partial\left(\rho^S\left(1-\varepsilon\right)T\right)}{\partial t}+\hat{C}_p^{gas}\nabla\left(\rho^G\mathbf{u}T\right)=-\nabla q-\left.\frac{\partial\ln\rho^G}{\partial\ln T}\right|_p\frac{Dp}{Dt}+\dot{Q}_R-\sum_{k=1}^{NC_{gas}}\hat{H}_k\nabla j_k \tag{5}$$

In order to estimate the effective solid and gaseous volume in every computational cell, the porosity within the particle is determined as follows (Eq(6)).

$$\varepsilon(t)=1-\frac{m^S(t)}{\rho^S V} \tag{6}$$

$\varepsilon=0$ when only the solid phase is present and $\varepsilon=1$ if there is no solid.

The source term $\mathbf{S}$ showed in the equation for conservation of momentum (Eq(2)) is computed according the Darcy-Forchheimer Law (Eq. (7)).

$$\mathbf{S}=-\left(\mu\mathbf{D}+\frac{1}{2}\rho^G\left|u_{kk}\right|\mathbf{F}\right)\mathbf{u} \tag{7}$$

$\mathbf{S}$ is composed of two terms, a viscous loss term and an inertial loss term, creating a pressure drop that is proportional to the velocity and velocity squared, respectively.

2.2 Governing equations of fluid phase

The reactive flows under investigation are mathematically described by the conservation equations for continuous, multicomponent, compressible, thermally-perfect mixtures of gases. The conservation equations of total mass, mixture momentum, individual species mass fractions and mixture energy are reported in the following for a Newtonian fluid:

$$\frac{\partial}{\partial t}\left(\rho^G \varepsilon\right)+\nabla\left(\rho^G \mathbf{u}\right)=0 \tag{8}$$

$$\frac{\partial}{\partial t}\left(\rho^G \mathbf{u}\right)+\nabla\left(\rho^G \mathbf{u}\mathbf{u}\right)=-\nabla p+\nabla\cdot\left[\mu\left(\nabla\mathbf{u}+\nabla\mathbf{u}^T\right)-\frac{2}{3}\mu\left(\nabla\mathbf{u}\right)\mathbf{I}\right]+\rho^G\mathbf{g} \tag{9}$$

$$\frac{\partial}{\partial t}\left(\rho^G \omega_k\right)+\nabla\left(\rho^G \omega \mathbf{u}\right)=-\nabla j_k+\dot{\Omega}_k \qquad k=1,\ldots,NC_{gas} \tag{10}$$

$$\hat{C}_p\frac{\partial\left(\rho^G T\right)}{\partial t}+\hat{C}_p\nabla\left(\rho^G\mathbf{u}T\right)=-\nabla q-\left.\frac{\partial\ln\rho^G}{\partial\ln T}\right|_p\frac{Dp}{Dt}+\dot{Q}_R-\sum_{k=1}^{NC_{gas}}\hat{H}_k\nabla j_k \tag{11}$$

2.3 Interface boundary conditions

The multiregion approach requires the definition of proper boundary conditions at the interfaces between the different regions of the domain, which are characterized by the same value of mass, heat and convective fluxes and, at the same time, by the same local value of the species mass fractions, temperature and velocity as explained in Eq(12-14). The nomenclature is summarized in Table 1.

- Temperature boundary conditions

$$\begin{cases} -\lambda \nabla T\big|_{fluid} = \lambda \nabla T\big|_{solid} + \dot{Q}_{rad} \\ T_I^{fluid} = T_I^{solid} \end{cases} \tag{12}$$

- Gas species boundary conditions

$$\begin{cases} -\rho^G \Gamma \nabla \omega_k\big|_{fluid} = -\rho^G \Gamma \nabla \omega_k\big|_{solid} \\ \omega_{k,I}^{\text{fluid}} = \omega_{k,\text{I}}^{solid} \end{cases} \qquad k = 1, ..., NC_{gas} \tag{13}$$

- Velocity boundary conditions

$$\begin{cases} \rho \mathbf{u}\big|_{fluid} = \rho \mathbf{u}\big|_{solid} \\ \mathbf{u}_I^{fluid} = \mathbf{u}_I^{solid} \end{cases} \tag{14}$$

In the equations reported above, t is the time, p and T are the pressure and the temperature, $\mathbf{u}$ the velocity vector, $\mathbf{g}$ the acceleration vector due to gravity and $\mathbf{I}$ the identity tensor. ρ^G and ρ^S are the density of gas and solid phase, j_k are the diffusion fluxes computed according the Fick's Law, $\dot{\Omega}_k$ and $\dot{\Omega}_j$ are the reaction rates for the gas and solid species, respectively. $\hat{C}_p^{gas}$ is the gas mixture specific heat at constant pressure, $\hat{C}^{solid}$ is the solid specific heat, q is the conductive flux computed according the Fourier's Law, $\frac{Dp}{Dt}$ is the pressure substantial derivative, $\dot{Q}_R$ is the reaction heat. and λ refer to the diffusivity coefficient and thermal conductivity, respectively. $\dot{Q}_{rad}$ accounts to the radiative flux. The subscript k refers to the individual gas-phase species and ω_k is the mass fraction. On the other hand, the subscript j refers to the individual solid-phase species and ω_j is the mass fraction.

3. Results and discussion

In this section, we perform a test case for the pyrolysis of a sugarcane-bagasse particle under the operating conditions encountered in a drop tube reactor (Levendis et al., 2011). This is a preliminary simulation of the new CFD code developed. Of course, in the future additional, more complex cases have to be tested, both in terms of numerical verification and in terms of validation with respect to the experimental measurements.

The devolatilization of the biomass is considered a straightforward combination of the pyrolysis of four reference components: as already discussed elsewhere (Debiagi et al., 2015). The multistep kinetic scheme used in current study for the biomass pyrolysis is the POLIMI_BM_1402 that describe the pyrolysis of the biomass through 42 species and 24 reactions (Corbetta et al., 2014).

Moreover, the combustion and the secondary pyrolysis of the nascent volatiles released from biomass has been modeled with a reduced mechanism starting from the comprehensive POLIMI_BIO_1311 kinetic mechanism (7000 reactions and 202 species). This reduced mechanism (70 species and 1019 reactions) has been obtained following the procedure describe elsewhere (Stagni et al., 2016) able to guarantee the correct trade-off between numerical accuracy and computational effort required in CFD simulations.

A schematic view of the overall computational grid is presented in Figure 1, while the operating conditions of the simulation are reported in Table 1.

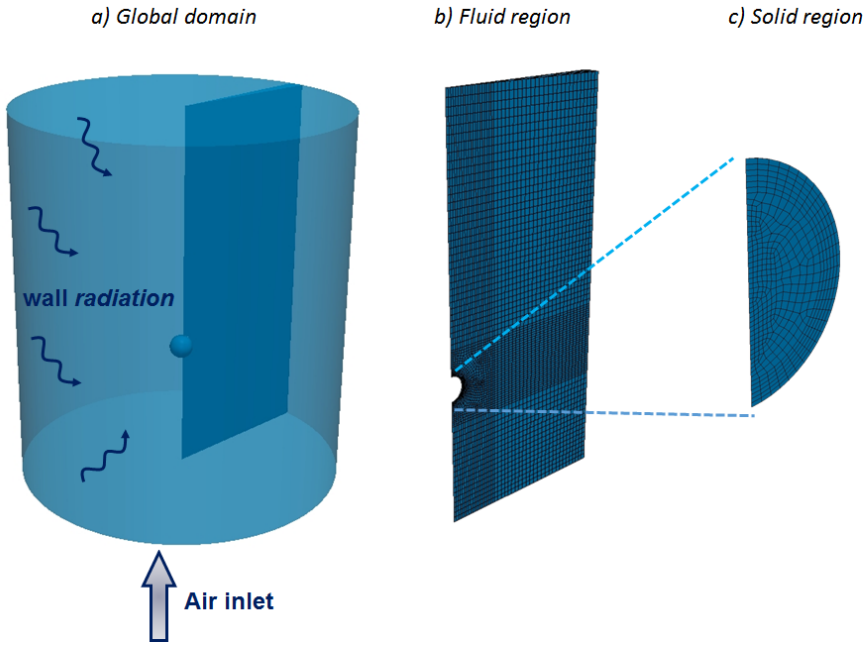

Figure 1: Computational mesh used for the simulation. a) global domain; b) fluid region (4099 cells); c) solid region (458 cells)

Exploiting the symmetry of the domain (Fig. 1 (a)), it is possible to consider only a slice of overall reactor with a width of 5°.The resulted 2D mesh (Fig. 1 (b-c)) has 4557 cells and has been considered fine enough for the test-case here proposed. Air is injected at 1350 K with a velocity of 4.5 cm/s. The temperature wall is set to 1400 K and, as sketched in Figure 1, the effect of the radiating wall has been take into account, too. It leads to a higher particle heating rate, in order of 10^5 K/s.

Table 1: Operating conditions

Operating conditions	
Particle diameter [μm]	100
Reactor diameter [mm]	0.7
Reactor height [mm]	1.6
Inlet mass fraction [%]	
Cellulose	52.7
Hemicellulose	28.6
Lignins	14.7
Ash	4

Figure 2 shows the temperature maps both in fluid and solid region at three different times during the transient. As expected, the biomass particle releases volatiles during the pyrolysis that generate a typical fuel particle envelope flame. After the ignition, shown in Figure 2 (panel b), a remarkable thermal back-diffusion is registered in the fluid domain that strongly affects the particle heating, Figure 2 (panel c).

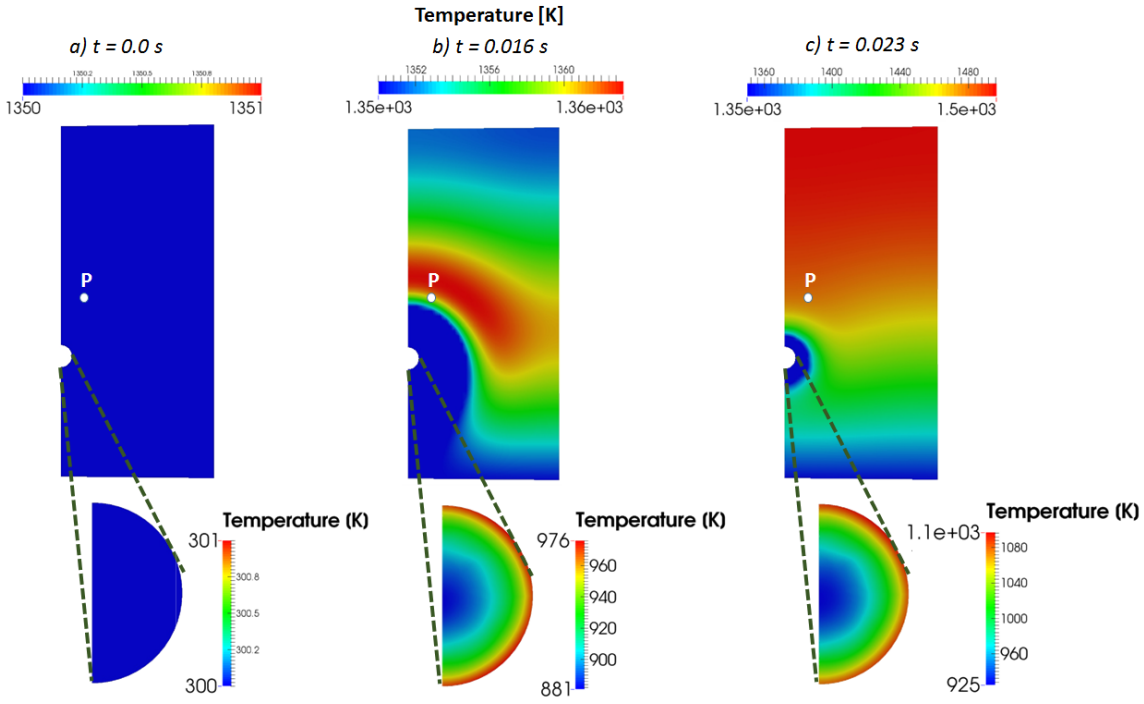

Figure 2: Cross-section temperature profile (z=0) both in the fluid region (top) and in the solid one (bottom) for different times. Panel a: 0.0 s, panel b: 0.016 s, panel c: 0.023 s.

Despite the small particle dimension, significant internal temperature gradients are highlighted inside the solid. This is due to the higher heating rate that leads to higher Biot number, order of 10^2.
Figure 3-4 show the evolution of the main fields calculated in the fluid and solid domain respectively.

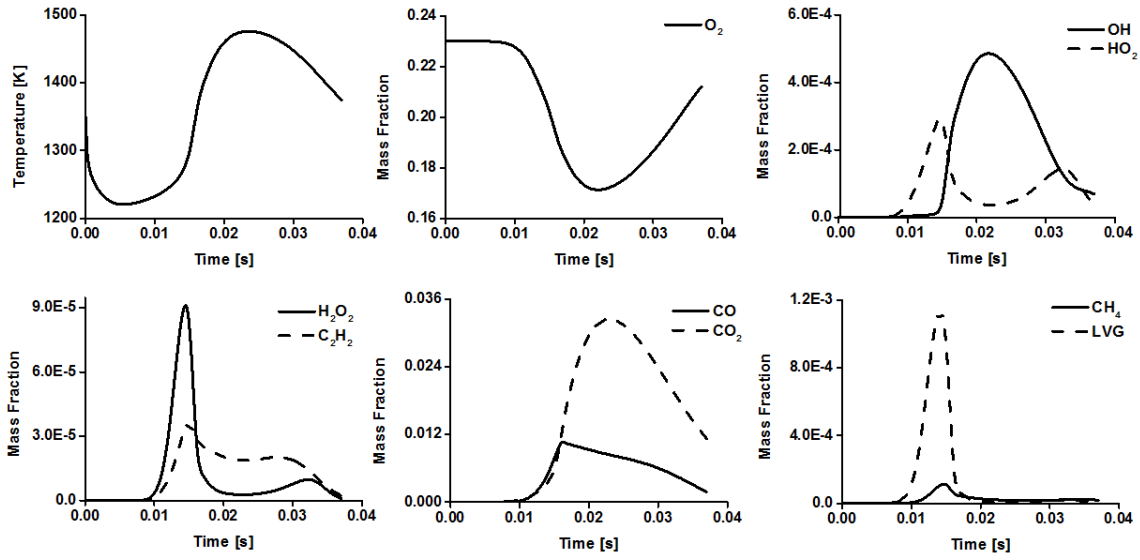

Figure3: Temperature and main gas and radical species profiles in the fluid region. Plot refers to the temporal trends at the point P highlighted in Figure 2

The temperature profile in the fluid region shows the presence of different thermal regimes during the pyrolysis. Temperature first decreases due to the heating of the colder solid particle, originally at room temperature. Once the pyrolysis starts, the ignition of the nascent volatiles occurs and the temperature strongly increases until reaching a maximum value at about 0.025 s. From this point, temperature decreases

again because of the flame extinction. The volatiles released in the gas phase initially form HO_2 and H_2O_2 due to the relatively low temperature around the particle. The decomposition of H_2O_2 leads to auto-ignition and transition to the high temperature combustion regime, where OH radicals promote the oxidation of volatiles to CO and CO_2.
The profiles inside the particle are coherent with evolution in the fluid domain as shown in Figure 4. Both the pressure and velocity fields reach the maximum value at about 0.025 s and at the same time almost all the biomass is consumed as highlighted by the cellulose and hemicellulose trends.

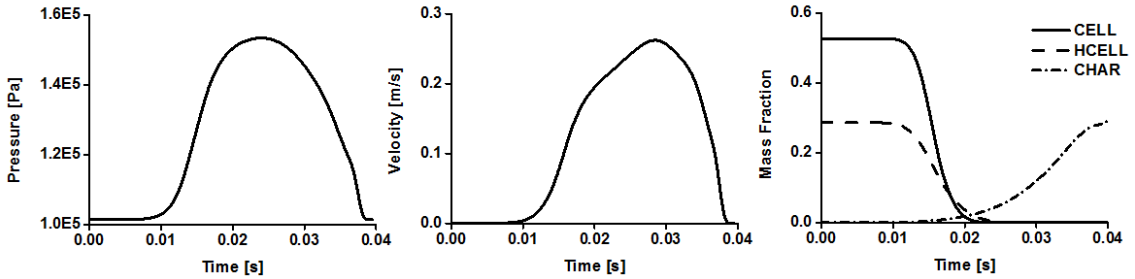

Figure4: Pressure, velocity and main species profiles in the solid region. Plot refers to the temporal trends at the centre of biomass particle

4. Conclusions

A general and comprehensive CFD model for the biomass pyrolysis has been developed in this work. A multiregion approach has been used to account internal mass/energy transport both inside the particle and at reactor scale where combustion and secondary pyrolysis of nascent volatiles occurs.
Pyrolysis of isolated particle of sugarcane-bagasse was investigated through complex kinetic mechanism in order to study the establishment of envelope particle flame. The model turns to be in reasonable agreement with the expected trends and paves the way to be very useful in the modelling of thermochemical processes that involve solid particles. The study of the effect of particle shrinking and the temporal evolution of physical parameters such as thermal conductivity and porosity will be a key area of possible improvement in the future in order to have a deep understanding all the fundamental phenomena that affects thermal degradation of solid fuels.

Acknowledgement

The authors gratefully acknowledge the activity of Andrea Mazzucotelli and Loris Torregiani.

References

Bates, R. B. & Ghoniem, A. F. 2014. Modeling kinetics-transport interactions during biomass torrefaction: The effects of temperature, particle size, and moisture content. *Fuel,* 137**,** 216-229.
Corbetta, M., Frassoldati, A., Bennadji, H., Smith, K., Serapiglia, M. J., Gauthier, G., Melkior, T., Ranzi, E. & Fisher, E. M. 2014. Pyrolysis of centimeter-scale woody biomass particles: Kinetic modeling and experimental validation. *Energy and Fuels,* 28**,** 3884-3898.
Debiagi, P. E. A., Pecchi, C., Gentile, G., Frassoldati, A., Cuoci, A., Faravelli, T. & Ranzi, E. 2015. Extractives Extend the Applicability of Multistep Kinetic Scheme of Biomass Pyrolysis. *Energy and Fuels,* 29**,** 6544-6555.
Gentile, G., Cuoci, A., Frassoldati, A., Faravelli, T. & Ranzi, E. 2015. A comprehensive CFD model for the biomass pyrolysis. *Chemical Engineering Transactions.*
Levendis, Y. A., Joshi, K., Khatami, R. & Sarofim, A. F. 2011. Combustion behavior in air of single particles from three different coal ranks and from sugarcane bagasse. *Combustion and Flame,* 158**,** 452-465.
Maffei, T., Gentile, G., Rebughini, S., Bracconi, M., Manelli, F., Lipp, S., Cuoci, A. & Maestri, M. 2016. A multiregion operator-splitting CFD approach for coupling microkinetic modeling with internal porous transport in heterogeneous catalytic reactors. *Chemical Engineering Journal,* 283**,** 1392-1404.
Openfoam. Available: http://www.openfoam.org/ [Accessed 28.01 2016].
Stagni, A., Frassoldati, A., Cuoci, A., Faravelli, T. & Ranzi, E. 2016. Skeletal mechanism reduction through species-targeted sensitivity analysis. *Combustion and Flame,* 163**,** 382-393.